

ON THE ENERGY-MOMENTUM CONSERVING INTEGRATION OF LARGE DEFORMATION CONTACT PROBLEMS

Christian Hesch^{*}, Peter Betsch[†]

Chair of Computational Mechanics, Department of Mechanical Engineering,
University of Siegen, Paul-Bonatz-Str. 9-11, D-57068 Siegen, Germany
web page: <http://www.uni-siegen.de/fb11/nm>
e-mail: ^{*}hesch@imr.mb.uni-siegen.de, [†]betsch@imr.mb.uni-siegen.de

Keywords: frictionless contact problems, conserving time integration, discrete gradient, mortar method

Abstract. *Dynamic contact problems in elasticity are dealt with in the framework of nonlinear finite element methods. To this end, the mortar method is applied to take into account the constraint of impenetrability. A new energy-momentum conserving time-stepping scheme for the mortar contact formulation is presented. The proposed method relies on a reparametrization of the contact constraints in terms of specific invariants. In this way, the symmetry properties of the underlying finite-dimensional mechanical system can be naturally accounted for by exploiting Cauchy's representation theorem. For the time discretization of the contact forces emanating from the mortar formulation the notion of a discrete gradient is applied.*

1 Introduction

In the present work large deformation contact problems of elastic bodies are addressed within a nonlinear finite element framework. That is, the underlying continuum formulation of flexible bodies relies on nonlinear strain measures and provides the possibility to incorporate arbitrary phenomenological constitutive models. We refer to the books by Laursen [14] and Wriggers [27] for a survey of previous developments in this field.

We choose to use hyperelastic material behavior so that the resulting semi-discrete, finite-dimensional system can be classified as Hamiltonian system with symmetry. The momentum maps (i.e. linear and angular momenta) associated with specific symmetries are known to be conserved quantities. Under the assumption of frictionless contact the total energy is a conserved quantity too.

Energy-momentum conserving schemes (and energy decaying variants thereof) have previously been developed in the framework of nonlinear elastodynamics in order to meet the numerical stability requirements of finite-deformation problems, see, for example, Simo & Tarnow [23], Gonzalez & Simo [12], Bauchau & Bottasso [3], Betsch & Steinmann [6] and the references cited therein.

Finite deformation contact problems put even higher demands on the numerical stability properties of time-stepping schemes. It is thus not surprising that recently published works aim at the extension of energy-momentum schemes to the realm of contact/impact problems. To this end Laursen & Chawla [15] enforce the discrete gap rate rather than the constraint of impenetrability. Similarly, Armero & Petöcz [2] modify the contact constraint to achieve the desired conservation properties. Consequently, in both works the impenetrability condition is violated in general. Alternatively, Laursen & Love [16] enforce the constraint of impenetrability and achieve algorithmic energy conservation by introducing a so-called discrete contact velocity. However, this approach requires the solution of quadratic equations which turn out to be unsolvable in some events.

It is important to note that the previous developments of energy-momentum schemes have been made exclusively in the context of the node-to-segment (NTS) formulation of the contact problem. Alternatively, recent approaches resolve the spatial contact problem in the framework of the mortar method, see, for example, Hübner & Wohlmuth [13], Puso & Laursen [20] and Yang et al. [28]. Originally, mortar methods have been developed for domain decomposition problems, see Wohlmuth [26]. Unlike the popular NTS method, the mortar-based approach typically passes the patch test and is characterized by enhanced robustness.

In the present work we aim at the design of energy-momentum schemes for contact problems in the framework of the mortar formulation. From the outset we regard the semi-discrete contact problem as finite-dimensional Hamiltonian system subject to (holonomic) contact constraints. Accordingly, the equations of motion assume the form of differential-algebraic equations (DAEs). Energy-momentum schemes emanating from the direct discretization of the DAEs have been recently developed, see Gonzalez [10] and Betsch & Steinmann [7]. Based on these developments our approach to the design of energy-momentum schemes makes use of the invariance properties of the discrete contact constraints by exploiting the representation theorem due to Cauchy.

An outline of the rest of the paper is as follows. Section 2 deals with the Hamiltonian formulation of semi-discrete elastodynamics. In this connection, the incorporation of algebraic

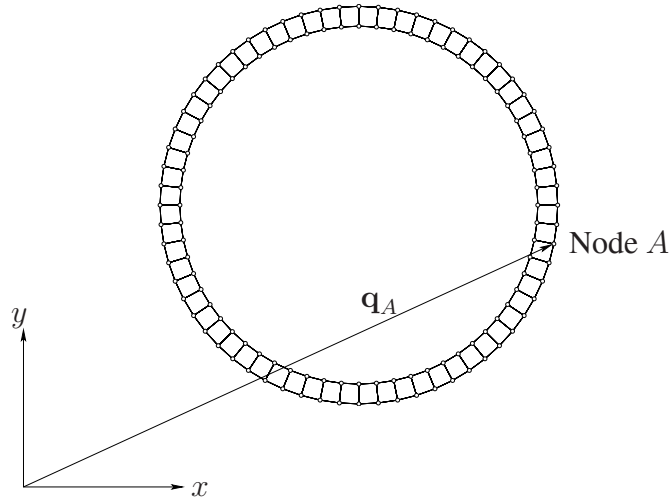


Figure 1: Planar ($n_{dim} = 2$) sketch of a free semi-discrete body.

constraints is treated and the relevant conservation properties are outlined. In Section 3 the energy-momentum conserving discretization of the underlying DAEs is dealt with. In particular, the notion of a discrete gradient is introduced in conjunction with Cauchy’s representation theorem. In Section 4 the present approach is particularized to the mortar formulation of the contact problem. After the treatment of a representative numerical example in Section 5, conclusions are drawn in Section 6.

2 Hamiltonian formulation of semi-discrete elastodynamics

We start with the space finite element discretization of nonlinear elastodynamics. In particular, we aim at the Hamiltonian formulation of the resulting semi-discrete problem. Further details of the present discretization approach may be found in Simo [21, CHAPTER IV] and the works cited therein.

2.1 The free semi-discrete elastic body

We first focus on the space discretization of the free elastic body (i.e. pure Neumann boundary conditions). Let \mathcal{B} be a regular region in n_{dim} -dimensional Euclidean space ($n_{dim} \leq 3$) occupied by the reference configuration of the elastic body. Furthermore, let $\mathbb{I} = [0, T]$ denote the time interval of interest. From a kinematic point of view the standard displacement-based finite element approach employs an approximation of the deformation field $\varphi : \mathcal{B} \times \mathbb{I} \rightarrow \mathbb{R}^{n_{dim}}$ of the form

$$\varphi(\mathbf{X}, t) = \sum_{A=1}^{n_{node}} N_A(\mathbf{X}) \mathbf{q}_A(t) \quad (1)$$

Within the material (or Lagrangian) description of motion $\varphi(\mathbf{X}, t)$ describes the position of material point \mathbf{X} of body \mathcal{B} at time t . Moreover, $N_A : \mathcal{B} \rightarrow \mathbb{R}$ are global shape functions associated with the nodes $A = 1, \dots, n_{node}$ and $\mathbf{q}_A : \mathbb{I} \rightarrow \mathbb{R}^{n_{dim}}$ denotes the position vector at time $t \in \mathbb{I}$ of the nodal point A (Fig. 1). Accordingly, possible configurations of the semi-discrete dynamical system at hand are characterized by

$$\mathbf{q} = (\mathbf{q}_1, \dots, \mathbf{q}_{n_{node}}) \in \mathbb{R}^{n_{dof}} \quad (2)$$

where $n_{dof} = n_{dim} \cdot n_{node}$. The material velocity is defined by $\mathbf{v} = \partial\varphi/\partial t = \dot{\varphi}$ such that the finite element approximation implies

$$\mathbf{v}(\mathbf{X}, t) = \sum_{A=1}^{n_{node}} N_A(\mathbf{X}) \mathbf{v}_A(t) \quad (3)$$

with $\mathbf{v}_A = \dot{\mathbf{q}}_A$. Moreover, the finite element approximation (1) gives rise to the discrete deformation gradient

$$\mathbf{F} = \frac{\partial\varphi}{\partial\mathbf{X}} = \sum_{A=1}^{n_{node}} \mathbf{q}_A \otimes \nabla N_A(\mathbf{X}) \quad (4)$$

Then the discrete version of the deformation tensor (or right Cauchy-Green tensor) $\mathbf{C} = \mathbf{F}^T \mathbf{F}$ can be written as

$$\mathbf{C} = \sum_{A,B=1}^{n_{node}} \mathbf{q}_A \cdot \mathbf{q}_B \nabla N_A \otimes \nabla N_B \quad (5)$$

Hyperelastic material behavior is modeled by means of a scalar-valued strain energy density function $W(\mathbf{C})$ such that the second Piola-Kirchhoff stress tensor can be calculated via

$$\mathbf{S} = 2DW(\mathbf{C}) \quad (6)$$

where $DW(\mathbf{C}) = \partial W/\partial\mathbf{C}$. Then the discrete strain energy function is given by

$$V^{int}(\mathbf{q}) = \int_{\mathcal{B}} W(\mathbf{C}) dV \quad (7)$$

For simplicity we assume that the external forces acting on the body can be derived from a potential function

$$V^{ext} = - \int_{\mathcal{B}} \varrho_R \mathbf{b} \cdot \boldsymbol{\varphi} dV - \int_{\partial\mathcal{B}_\sigma} \bar{\mathbf{t}} \cdot \boldsymbol{\varphi} dA \quad (8)$$

where $\varrho_R : \mathcal{B} \rightarrow \mathbb{R}_+$ denotes the reference mass density, $\mathbf{b} : \mathcal{B} \times \mathbb{I} \rightarrow \mathbb{R}^{n_{dim}}$ is the applied body force and $\bar{\mathbf{t}}$ is the prescribed traction boundary condition on $\partial\mathcal{B}_\sigma \times \mathbb{I}$. In view of (1) one obtains

$$V^{ext}(\mathbf{q}) = - \sum_{A=1}^{n_{node}} \mathbf{q}_A \cdot \mathbf{F}_A^{ext} \quad (9)$$

with prescribed external nodal forces

$$\mathbf{F}_A^{ext} = \int_{\mathcal{B}} N_A \varrho_R \mathbf{b} dV + \int_{\partial\mathcal{B}_\sigma} N_A \bar{\mathbf{t}} dA \quad (10)$$

The kinetic energy of the body at time t is given by

$$T = \frac{1}{2} \int_{\mathcal{B}} \varrho_R \mathbf{v} \cdot \mathbf{v} dV \quad (11)$$

such that substitution from (3) into (11) leads to

$$T(\mathbf{v}) = \frac{1}{2} \sum_{A,B=1}^{n_{node}} M_{AB} \mathbf{v}_A \cdot \mathbf{v}_B = \frac{1}{2} \mathbf{v} \cdot \mathbf{M} \mathbf{v} \quad (12)$$

where

$$M_{AB} = \int_{\mathcal{B}} \varrho_R N_A N_B dV \quad (13)$$

are the coefficients of the consistent mass matrix. Note that \mathbf{M} consists of diagonal sub-matrices $\mathbf{M}_{AB} = M_{AB} \mathbf{I}_{n_{dim}}$ with $A, B = 1, \dots, n_{node}$. The Lagrangian of the finite-dimensional dynamical system under consideration is given by $L(\mathbf{q}, \mathbf{v}) = T(\mathbf{v}) - (V^{int}(\mathbf{q}) + V^{ext}(\mathbf{q}))$. To perform the transition to the Hamiltonian formulation we introduce the conjugate momenta

$$\mathbf{p} = \frac{\partial L}{\partial \mathbf{v}} = \mathbf{M} \mathbf{v} \quad (14)$$

Then the Hamiltonian function follows from the Legendre transformation of $L(\mathbf{q}, \mathbf{v})$ with respect to \mathbf{v} as $H(\mathbf{q}, \mathbf{p}) = \mathbf{p} \cdot \mathbf{v} - L(\mathbf{q}, \mathbf{v})$, with the velocities \mathbf{v} being replaced by the momenta in (14). Accordingly, the Hamiltonian of the free semi-discrete elastic body can be written in the form

$$H(\mathbf{q}, \mathbf{p}) = \frac{1}{2} \mathbf{p} \cdot \mathbf{M}^{-1} \mathbf{p} + V^{int}(\mathbf{q}) + V^{ext}(\mathbf{q}) \quad (15)$$

Consequently, the equations of motion can be written in canonical Hamiltonian form

$$\begin{aligned} \dot{\mathbf{q}} &= \frac{\partial H}{\partial \mathbf{p}} = \mathbf{M}^{-1} \mathbf{p} \\ \dot{\mathbf{p}} &= -\frac{\partial H}{\partial \mathbf{q}} = \mathbf{F}^{ext} - \mathbf{F}^{int}(\mathbf{q}) \end{aligned} \quad (16)$$

In this connection, the internal forces are given by

$$\mathbf{F}^{int}(\mathbf{q}) = \nabla V^{int}(\mathbf{q}) \quad (17)$$

A more compact description of the equations of motion can be achieved by introducing the vector of phase space coordinates

$$\mathbf{z} = (\mathbf{q}, \mathbf{p}) \in \mathbb{R}^{2n_{dof}} \quad (18)$$

Then the equations of motion pertaining to the semi-discrete free elastic body can alternatively be written as

$$\dot{\mathbf{z}} = \mathbb{J} \nabla H(\mathbf{z}) \quad (19)$$

In the last equation $\mathbb{J} \in \mathbb{R}^{2n_{dof} \times 2n_{dof}}$ is the canonical symplectic matrix

$$\mathbb{J} = \begin{bmatrix} \mathbf{0} & \mathbf{I} \\ -\mathbf{I} & \mathbf{0} \end{bmatrix} \quad (20)$$

where \mathbf{I} and $\mathbf{0}$ are the $n_{dof} \times n_{dof}$ identity and zero matrices. Note that $\mathbb{J}^T = \mathbb{J}^{-1} = -\mathbb{J}$ and $\mathbb{J}^2 = -\mathbb{I}$, where \mathbb{I} denotes the $(2n_{dof} \times 2n_{dof})$ identity matrix.

2.2 Constrained semi-discrete elastic bodies

We next focus on specific boundary conditions which restrict the motion of the semi-discrete elastic body. These restrictions can be characterized by geometric constraints acting on the boundary nodes of the discrete system at hand. In particular, we distinguish between Dirichlet-type boundary conditions and constraints due to contact. For the present purposes it suffices to consider the planar two-body contact problem (Fig. 2).

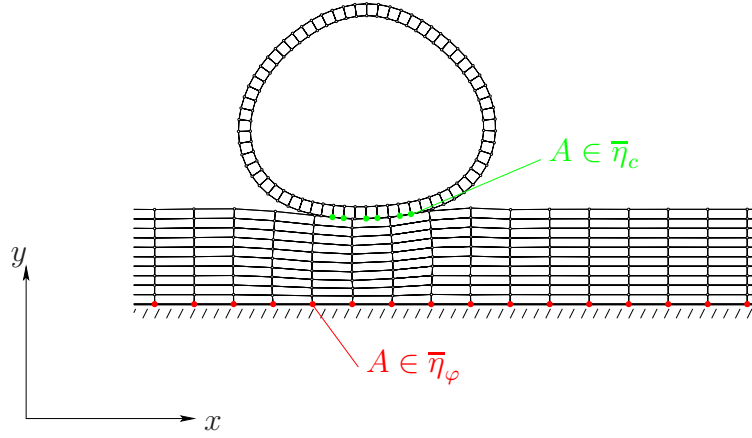


Figure 2: The planar two-body contact problem.

Assume that n_{node} denotes the total number of nodes due to the space discretization of the two elastic bodies, so that $\eta = \{1, \dots, n_{node}\}$ is the set of node numbers associated with the discrete two-body system. Further let $\bar{\eta} \subset \eta$ be the set of node numbers lying on the boundaries of the two-body system. The relevant boundary conditions can be characterized by algebraic constraints of the form

$$\Phi(\mathbf{q}) = \mathbf{0} \quad (21)$$

In the case of Dirichlet-type boundary conditions we have

$$\mathbf{q}_A(t) = \bar{\varphi}(\mathbf{X}_A, t), \quad \text{for } A \in \bar{\eta}_\varphi \quad (22)$$

where $\bar{\varphi}_t$ is prescribed and $\bar{\eta}_\varphi \subset \bar{\eta}$ is the set of node numbers belonging to the Dirichlet boundary. Similarly, if the two bodies are in contact and provided that ‘active’ nodes $A \in \bar{\eta}_c \subset \bar{\eta} - \bar{\eta}_\varphi$ lying on the contact surface have been detected, additional constraints of the form (21) arise (see Section 4 for further details). Due to the presence of the constraints (21), the equations of motion can now be written in the form

$$\begin{aligned} \dot{\mathbf{q}} &= \frac{\partial H}{\partial \mathbf{p}} \\ \dot{\mathbf{p}} &= -\frac{\partial H}{\partial \mathbf{q}} - D\Phi(\mathbf{q})^T \boldsymbol{\lambda} \\ \mathbf{0} &= \Phi(\mathbf{q}) \end{aligned} \quad (23)$$

where $\Phi(\mathbf{q}) \in \mathbb{R}^m$ are the relevant constraint functions, $D\Phi(\mathbf{q})$ is the corresponding constraint Jacobian and $\boldsymbol{\lambda} \in \mathbb{R}^m$ are Lagrange multipliers which determine the size of the constraint forces in (23)₂. Similar to (19), the set of differential-algebraic equations (DAEs) in (23) can be rewritten in compact form by introducing the augmented Hamiltonian

$$\mathcal{H}_\lambda(\mathbf{z}) = \frac{1}{2} \mathbf{p} \cdot \mathbf{M}^{-1} \mathbf{p} + \mathcal{V}_\lambda(\mathbf{q}) \quad (24)$$

where

$$\mathcal{V}_\lambda(\mathbf{q}) = V^{int}(\mathbf{q}) + V^{ext}(\mathbf{q}) + \boldsymbol{\lambda} \cdot \Phi(\mathbf{q}) \quad (25)$$

is an augmented potential function. Now the differential part of the DAEs can be written as

$$\dot{\mathbf{z}} = \mathbb{J}\nabla\mathcal{H}_\lambda(\mathbf{z}) \quad (26)$$

which, of course, has to be supplemented with the algebraic constraints (23)₃.

2.3 Conservation properties of the semi-discrete system

We next focus on the conservation properties relevant for the constrained finite-dimensional mechanical system under consideration. Our goal is the subsequent design of time-stepping schemes which inherit these conservation properties from the semi-discrete system. Since algorithmic conservation of total linear momentum is rather trivial we focus on the conservation properties associated with the total angular momentum and the total energy.

2.3.1 Conservation of the total angular momentum

In this section we elaborate on the connection between specific symmetry properties of the augmented Hamiltonian (24) and associated momentum maps (see Marsden & Ratiu [17] for more background information on these issues). In particular, we focus on the rotational invariance of the augmented Hamiltonian which implies conservation of the total angular momentum. Accordingly, assume that the augmented Hamiltonian is invariant under rotations such that

$$\mathcal{H}_\lambda(\mathbf{Q} \circ \mathbf{z}) := \mathcal{H}_\lambda(\mathbf{Q}\mathbf{q}_1, \dots, \mathbf{Q}\mathbf{q}_N, \mathbf{Q}\mathbf{p}_1, \dots, \mathbf{Q}\mathbf{p}_N) \equiv \mathcal{H}_\lambda(\mathbf{z}) \quad (27)$$

for all proper orthogonal matrices $\mathbf{Q} \in SO(3)$, where $SO(3)$ denotes the rotation group. A one-parameter group of rotation matrices can be written in the form $\mathbf{Q}_\varepsilon = \exp(\varepsilon\hat{\boldsymbol{\xi}}) \in SO(3)$ where $\hat{\boldsymbol{\xi}} \in so(3)$ is a skew-symmetric matrix. In the present case a closed-form expression of $\exp(\varepsilon\hat{\boldsymbol{\xi}})$ is given by the Rodrigues formula (see, for example, Marsden & Ratiu [17, Chapter 9]). The invariance property (27) implies

$$0 = \left. \frac{d}{d\varepsilon} \right|_{\varepsilon=0} \mathcal{H}_\lambda(\exp(\varepsilon\hat{\boldsymbol{\xi}}) \circ \mathbf{z}) = \nabla\mathcal{H}_\lambda(\mathbf{z}) \cdot \left. \frac{d}{d\varepsilon} \right|_{\varepsilon=0} \exp(\varepsilon\hat{\boldsymbol{\xi}}) \circ \mathbf{z} = \nabla\mathcal{H}_\lambda(\mathbf{z}) \cdot \boldsymbol{\xi}_P(\mathbf{z}) \quad (28)$$

where $\boldsymbol{\xi}_P(\mathbf{z})$ denotes the infinitesimal generator. The associated momentum map is defined by

$$\boldsymbol{\xi}_P(\mathbf{z}) = \mathbb{J}\nabla J_\xi(\mathbf{z}) \quad (29)$$

with

$$J_\xi(\mathbf{z}) = \mathbf{J}(\mathbf{z}) \cdot \boldsymbol{\xi} \quad (30)$$

Here, $\boldsymbol{\xi} \in \mathbb{R}^3$ is the axial vector of $\hat{\boldsymbol{\xi}}$ (i.e. $\hat{\boldsymbol{\xi}}\mathbf{a} = \boldsymbol{\xi} \times \mathbf{a}$ for all $\mathbf{a} \in \mathbb{R}^3$) and $\mathbf{J} \in \mathbb{R}^3$ is the total angular momentum given by

$$\mathbf{J}(\mathbf{z}) = \sum_{A=1}^{n_{node}} \mathbf{q}_A \times \mathbf{p}_A \quad (31)$$

Now a straightforward calculation yields

$$\begin{aligned} \frac{d}{dt} J_\xi(\mathbf{z}) &= \nabla J_\xi(\mathbf{z}) \cdot \dot{\mathbf{z}} \\ &= \nabla J_\xi(\mathbf{z}) \cdot \mathbb{J}\nabla\mathcal{H}_\lambda(\mathbf{z}) \\ &= \boldsymbol{\xi}_P(\mathbf{z}) \cdot \mathbb{J}^2 \nabla\mathcal{H}_\lambda(\mathbf{z}) \\ &= -\boldsymbol{\xi}_P(\mathbf{z}) \cdot \nabla\mathcal{H}_\lambda(\mathbf{z}) \\ &= 0 \end{aligned} \quad (32)$$

Thus rotational invariance of the augmented Hamiltonian implies conservation of the total angular momentum.

2.3.2 Conservation of the total energy

Due to the skew-symmetry of \mathbb{J} one obtains

$$\nabla \mathcal{H}_\lambda(\mathbf{z}) \cdot \dot{\mathbf{z}} = \nabla \mathcal{H}_\lambda(\mathbf{z}) \cdot \mathbb{J} \nabla \mathcal{H}_\lambda(\mathbf{z}) = 0 \quad (33)$$

With regard to (24) and (15), the augmented Hamiltonian can be written as

$$\mathcal{H}_\lambda(\mathbf{z}) = H(\mathbf{z}) + \boldsymbol{\lambda} \cdot \boldsymbol{\Phi}(\mathbf{q}) \quad (34)$$

Accordingly, (33) can be written in the form

$$\begin{aligned} \nabla H(\mathbf{z}) \cdot \dot{\mathbf{z}} + \boldsymbol{\lambda} \cdot D\boldsymbol{\Phi}(\mathbf{q})\dot{\mathbf{q}} &= 0 \\ \frac{d}{dt}H(\mathbf{z}) + \boldsymbol{\lambda} \cdot \frac{d}{dt}\boldsymbol{\Phi}(\mathbf{q}) &= 0 \end{aligned} \quad (35)$$

As a consequence of the geometric constraints (23)₃, the consistency condition $d\boldsymbol{\Phi}(\mathbf{q})/dt = \mathbf{0}$ has to be satisfied. Thus (35) yields $dH(\mathbf{z})/dt = 0$, which implies conservation of the total energy.

3 Energy-momentum scheme

We next outline the design of a time-stepping scheme which is able to reproduce for any step-size the crucial conservation properties summarized above.

Concerning the time discretization of the DAEs (23), we apply the Galerkin-based approach developed by Betsch & Steinmann [7]. To this end, we consider a characteristic time-step $\Delta t = t_{n+1} - t_n$ and restrict our attention to linear approximations (the so-called mG(1) method in [7]) of the form

$$\mathbf{z}^h(\alpha) = (1 - \alpha)\mathbf{z}_n + \alpha\mathbf{z}_{n+1} \quad \text{for } \alpha \in [0, 1] \quad (36)$$

In this connection all quantities at t_n , such as \mathbf{z}_n , can be regarded as being given. Note that (36) leads to a globally continuous approximation of the phase space coordinates. In contrast to that, the Lagrange multipliers are assumed to be piecewise constant in each time-step, i.e.

$$\boldsymbol{\lambda}^h = \boldsymbol{\lambda}_{n+1} \quad (37)$$

The mG(1) method yields

$$\mathbf{z}_{n+1} - \mathbf{z}_n = \Delta t \mathbb{J} \int_0^1 \nabla \mathcal{H}_{\lambda^h}(\mathbf{z}^h) d\alpha \quad (38)$$

It is shown in [7] that the application of a specific quadrature formula for the evaluation of the time integral in (38) has a strong impact on the conservation properties of the resulting time-stepping scheme. In the present work we choose

$$\int_0^1 \nabla \mathcal{H}_{\lambda^h}(\mathbf{z}^h) d\alpha \approx \bar{\nabla} \mathcal{H}_{\lambda_{n+1}}(\mathbf{z}_n, \mathbf{z}_{n+1}) \quad (39)$$

where $\bar{\nabla} \mathcal{H}_\lambda(z_n, z_{n+1})$ is a discrete gradient (or derivative) in the sense of Gonzalez [9]. It is shown in [9] that the discrete gradient can be designed such that the desired conservation properties are satisfied and specific consistency and accuracy requirements are met. To achieve this

goal we aim at a reparametrization of the augmented Hamiltonian which incorporates the invariance properties in a natural way. For example, assume that the rotational invariance property (27) holds and that the augmented Hamiltonian depends only on $\mathbb{S}(\mathbf{z})$, where

$$\mathbb{S}(\mathbf{z}) = \mathbb{S}(\mathbf{z}_1, \dots, \mathbf{z}_N) = \{\mathbf{y}_A \cdot \mathbf{y}_B, 1 \leq A \leq B \leq n_{node}, \mathbf{y}_A \in \{\mathbf{q}_A, \mathbf{p}_A\}\} \quad (40)$$

is the set of (quadratic) invariants of $\mathbf{z} \in \mathbb{R}^{2n_{dof}}$. It is worth mentioning that this approach is in accordance with Cauchy's representation theorem (see, for example, Truesdell & Noll [25, Sect. 11.]). Accordingly, the augmented Hamiltonian can now be written in the form

$$\mathcal{H}_\lambda(\mathbf{z}) = \tilde{\mathcal{H}}_\lambda(\boldsymbol{\pi}(\mathbf{z})) \quad (41)$$

where the vector of relevant invariants

$$\boldsymbol{\pi}(\mathbf{z}) = \begin{bmatrix} \pi_1(\mathbf{z}) \\ \vdots \\ \pi_d(\mathbf{z}) \end{bmatrix} \quad (42)$$

has been introduced. Note that the components $\pi_i(\mathbf{z})$ depend only on $\mathbb{S}(\mathbf{z})$. In the following we make use of Gonzalez' [9] definition of the discrete gradient. Accordingly, in the present context, the discrete gradient of the augmented Hamiltonian assumes the form

$$\boxed{\bar{\nabla} \mathcal{H}_\lambda(\mathbf{z}_n, \mathbf{z}_{n+1}) = D\boldsymbol{\pi}(\mathbf{z}_{n+\frac{1}{2}})^T \bar{\nabla} \tilde{\mathcal{H}}_\lambda(\boldsymbol{\pi}(\mathbf{z}_n), \boldsymbol{\pi}(\mathbf{z}_{n+1}))} \quad (43)$$

with

$$\begin{aligned} \bar{\nabla} \tilde{\mathcal{H}}_\lambda(\boldsymbol{\pi}_n, \boldsymbol{\pi}_{n+1}) &= \nabla \tilde{\mathcal{H}}_\lambda(\boldsymbol{\pi}_{n+\frac{1}{2}}) \\ &+ \frac{\tilde{\mathcal{H}}_\lambda(\boldsymbol{\pi}_{n+1}) - \tilde{\mathcal{H}}_\lambda(\boldsymbol{\pi}_n) - \nabla \tilde{\mathcal{H}}_\lambda(\boldsymbol{\pi}_{n+\frac{1}{2}}) \cdot (\boldsymbol{\pi}_{n+1} - \boldsymbol{\pi}_n)}{\|\boldsymbol{\pi}_{n+1} - \boldsymbol{\pi}_n\|^2} (\boldsymbol{\pi}_{n+1} - \boldsymbol{\pi}_n) \end{aligned} \quad (44)$$

and

$$\begin{aligned} \mathbf{z}_{n+\frac{1}{2}} &= \frac{1}{2}(\mathbf{z}_n + \mathbf{z}_{n+1}) \\ \boldsymbol{\pi}_{n+\frac{1}{2}} &= \frac{1}{2}(\boldsymbol{\pi}_n + \boldsymbol{\pi}_{n+1}) \end{aligned} \quad (45)$$

To summarize, the mG(1) method with quadrature formula (39) yields the following time-stepping scheme:

$$(H) = \begin{cases} \text{Let the initial values per time step } \mathbf{z}_n \text{ and the step-size } \Delta t \text{ be given. Find } \mathbf{z}_{n+1} \text{ and } \\ \boldsymbol{\lambda}_{n+1} \text{ as the solution of the algebraic system of equations} \\ \mathbf{z}_{n+1} = \mathbf{z}_n + \Delta t \mathbb{J} \bar{\nabla} \mathcal{H}_{\lambda_{n+1}}(\mathbf{z}_n, \mathbf{z}_{n+1}) \\ \mathbf{0} = \boldsymbol{\Phi}(\mathbf{q}_{n+1}) \end{cases} \quad (46)$$

In essence, the scheme (46) is equivalent to the method proposed by Gonzalez [10]. We further remark that in addition to the constraints on configuration level (46)₂, the constraints on momentum level, i.e. $d\boldsymbol{\Phi}(\mathbf{q})/dt = D\boldsymbol{\Phi}(\mathbf{q})\mathbf{M}^{-1}\mathbf{p} = \mathbf{0}$ can be enforced at the end of the time step by adjusting the GGL-type [8] technique to the present conserving framework, see [7] for further details. However, numerical tests revealed no significant improvement of the numerical performance which would justify the additional computational effort.

It is further worth noting that if a function $f(\mathbf{z})$ is merely quadratic it may be written as $f(\mathbf{z}) =$

$\tilde{f}(\boldsymbol{\pi}(\mathbf{z})) = \mathbf{a} \cdot \boldsymbol{\pi}(\mathbf{z})$, with constant $\mathbf{a} \in \mathbb{R}^d$. It can be easily verified that the corresponding discrete gradient is given by

$$\bar{\nabla} f(\mathbf{z}_n, \mathbf{z}_{n+1}) = D\boldsymbol{\pi}(\mathbf{z}_{n+\frac{1}{2}})^T \mathbf{a} = \nabla f(\mathbf{z}_{n+\frac{1}{2}}) \quad (47)$$

Accordingly, in this case the discrete gradient coincides with the standard gradient evaluated in $\mathbf{z}_{n+\frac{1}{2}}$.

3.1 Algorithmic conservation properties

Similar to the continuous case dealt with before, we next verify that the scheme (46) indeed satisfies the relevant conservation laws.

3.1.1 Algorithmic conservation of the total angular momentum

The fundamental theorem of calculus gives

$$\begin{aligned} J_\xi(\mathbf{z}_{n+1}) - J_\xi(\mathbf{z}_n) &= \int_0^1 \nabla J_\xi(\mathbf{z}^h(\alpha)) \cdot (\mathbf{z}^h(\alpha))' d\alpha \\ &= \int_0^1 \boldsymbol{\xi}_P(\mathbf{z}^h(\alpha)) d\alpha \cdot \mathbb{J}(\mathbf{z}_{n+1} - \mathbf{z}_n) \\ &= \boldsymbol{\xi}_P(\mathbf{z}_{n+\frac{1}{2}}) \cdot \mathbb{J}(\mathbf{z}_{n+1} - \mathbf{z}_n) \\ &= \boldsymbol{\xi}_P(\mathbf{z}_{n+\frac{1}{2}}) \cdot \mathbb{J}^2 \Delta t \bar{\nabla} \mathcal{H}_{\lambda_{n+1}}(\mathbf{z}_n, \mathbf{z}_{n+1}) \\ &= -\Delta t \bar{\nabla} \mathcal{H}_{\lambda_{n+1}}(\mathbf{z}_n, \mathbf{z}_{n+1}) \cdot \boldsymbol{\xi}_P(\mathbf{z}_{n+\frac{1}{2}}) \\ &= -\Delta t \bar{\nabla} \tilde{\mathcal{H}}_{\lambda_{n+1}}(\boldsymbol{\pi}(\mathbf{z}_n), \boldsymbol{\pi}(\mathbf{z}_{n+1})) \cdot D\boldsymbol{\pi}(\mathbf{z}_{n+\frac{1}{2}}) \boldsymbol{\xi}_P(\mathbf{z}_{n+\frac{1}{2}}) \\ &= 0 \end{aligned} \quad (48)$$

where, similar to (28), use has been made of the property

$$\mathbf{0} = \left. \frac{d}{d\varepsilon} \right|_{\varepsilon=0} \boldsymbol{\pi}(\exp(\varepsilon \hat{\boldsymbol{\xi}}) \circ \mathbf{z}) = D\boldsymbol{\pi}(\mathbf{z}) \boldsymbol{\xi}_P(\mathbf{z}) \quad (49)$$

which holds due to the rotational invariance of the vector-valued function $\boldsymbol{\pi}(\mathbf{z})$. Equation (48) corroborates algorithmic conservation of the total angular momentum.

3.1.2 Algorithmic conservation of the total energy

Similar to (33), in the discrete setting we get

$$\frac{1}{\Delta t} \bar{\nabla} \mathcal{H}_{\lambda_{n+1}}(\mathbf{z}_n, \mathbf{z}_{n+1}) \cdot (\mathbf{z}_{n+1} - \mathbf{z}_n) = \bar{\nabla} \mathcal{H}_{\lambda_{n+1}} \cdot \mathbb{J} \bar{\nabla} \mathcal{H}_{\lambda_{n+1}} = 0 \quad (50)$$

On the other hand, with regard to the discrete gradient (43), we obtain

$$\begin{aligned} \bar{\nabla} \mathcal{H}_{\lambda_{n+1}}(\mathbf{z}_n, \mathbf{z}_{n+1}) \cdot (\mathbf{z}_{n+1} - \mathbf{z}_n) &= \bar{\nabla} \tilde{\mathcal{H}}_{\lambda_{n+1}}(\boldsymbol{\pi}(\mathbf{z}_n), \boldsymbol{\pi}(\mathbf{z}_{n+1})) \cdot D\boldsymbol{\pi}(\mathbf{z}_{n+\frac{1}{2}}) \cdot (\mathbf{z}_{n+1} - \mathbf{z}_n) \\ &= \bar{\nabla} \tilde{\mathcal{H}}_{\lambda_{n+1}}(\boldsymbol{\pi}(\mathbf{z}_n), \boldsymbol{\pi}(\mathbf{z}_{n+1})) \cdot (\boldsymbol{\pi}(\mathbf{z}_{n+1}) - \boldsymbol{\pi}(\mathbf{z}_n)) \\ &= \tilde{\mathcal{H}}_{\lambda_{n+1}}(\boldsymbol{\pi}(\mathbf{z}_{n+1})) - \tilde{\mathcal{H}}_{\lambda_{n+1}}(\boldsymbol{\pi}(\mathbf{z}_n)) \\ &= \mathcal{H}_{\lambda_{n+1}}(\mathbf{z}_{n+1}) - \mathcal{H}_{\lambda_{n+1}}(\mathbf{z}_n) \\ &= H(\mathbf{z}_{n+1}) - H(\mathbf{z}_n) + \boldsymbol{\lambda}_{n+1} \cdot (\boldsymbol{\Phi}(\mathbf{q}_{n+1}) - \boldsymbol{\Phi}(\mathbf{q}_n)) \\ &= H(\mathbf{z}_{n+1}) - H(\mathbf{z}_n) \end{aligned} \quad (51)$$

where use has been made of (34), (44), (46) and the fact that the invariants $\pi(\mathbf{z})$ are quadratic functions. Comparison of (50) and (51) yields

$$H(\mathbf{z}_{n+1}) = H(\mathbf{z}_n) \quad (52)$$

which confirms algorithmic conservation of the total energy.

3.2 Final form of the energy-momentum scheme

We next exploit the specific (separable) form of the augmented Hamiltonian (24) to recast the energy-momentum scheme (46) in an alternative form which is especially well-suited for the computer implementation. With regard to (12), the kinetic energy in (24) can be written as

$$T(\mathbf{p}) = \frac{1}{2} \sum_{A,B=1}^{n_{node}} M_{AB}^{-1} \mathbf{p}_A \cdot \mathbf{p}_B \quad (53)$$

and is thus merely a quadratic function of the nodal momenta. In this connection, the inverse of the mass matrix is composed of diagonal sub-matrices $\mathbf{M}_{AB}^{-1} = M_{AB}^{-1} \mathbf{I}_{n_{dim}}$ ($A, B = 1, \dots, n_{node}$). The discrete gradient of the augmented Hamiltonian (43) can be written in simplified form

$$\bar{\nabla} \mathcal{H}_\lambda(\mathbf{z}_n, \mathbf{z}_{n+1}) = \begin{bmatrix} \bar{\nabla}_q \mathcal{V}_\lambda(\mathbf{q}_n, \mathbf{q}_{n+1}) \\ \bar{\nabla}_p T(\mathbf{p}_n, \mathbf{p}_{n+1}) \end{bmatrix} = \begin{bmatrix} \bar{\nabla}_q \mathcal{V}_\lambda(\mathbf{q}_n, \mathbf{q}_{n+1}) \\ \mathbf{M}^{-1} \mathbf{p}_{n+\frac{1}{2}} \end{bmatrix} \quad (54)$$

Accordingly, application of the discrete gradient is confined to the augmented potential function (25). That is, (43) boils down to

$$\boxed{\bar{\nabla}_q \mathcal{V}_\lambda(\mathbf{q}_n, \mathbf{q}_{n+1}) = D\boldsymbol{\pi}(\mathbf{q}_{n+\frac{1}{2}})^T \bar{\nabla} \tilde{\mathcal{V}}_\lambda(\boldsymbol{\pi}(\mathbf{q}_n), \boldsymbol{\pi}(\mathbf{q}_{n+1}))} \quad (55)$$

Now the energy-momentum scheme (46) gives rise to the following algorithmic problem:

$$(L) = \left\{ \begin{array}{l} \text{Let the initial values per time step } (\mathbf{q}_n, \mathbf{v}_n) \text{ and the step-size } \Delta t \text{ be given. Find} \\ (\mathbf{q}_{n+1}, \mathbf{v}_{n+1}) \text{ and } \boldsymbol{\lambda}_{n+1} \text{ as the solution of the algebraic system of equations} \\ \\ \mathbf{q}_{n+1} - \mathbf{q}_n = \frac{\Delta t}{2} (\mathbf{v}_n + \mathbf{v}_{n+1}) \\ \mathbf{M}(\mathbf{v}_{n+1} - \mathbf{v}_n) = -\Delta t \bar{\nabla}_q V(\mathbf{q}_n, \mathbf{q}_{n+1}) - \Delta t \sum_{l=1}^m (\lambda_l)_{n+1} \bar{\nabla}_q \Phi_l(\mathbf{q}_n, \mathbf{q}_{n+1}) \\ \mathbf{0} = \boldsymbol{\Phi}(\mathbf{q}_{n+1}) \end{array} \right. \quad (56)$$

In (56)₂ the potential energy function is given by $V(\mathbf{q}) = V^{int}(\mathbf{q}) + V^{ext}(\mathbf{q})$. We refer to [4] for details of the implementation of the energy-momentum scheme (56).

3.3 Application to planar problems

The application of the scheme (56) essentially depends on specific parametrizations of the discrete strain energy function $V^{int}(\mathbf{q})$ and the constraint functions $\Phi_l(\mathbf{q})$ in terms of appropriate invariants. We shall illustrate this procedure by considering planar problems, i.e. $n_{dim} = 2$ and $\mathbf{q}_A \in \mathbb{R}^2$ ($A \in \eta$).

As before, we focus on the case of rotational invariance. If a scalar-valued function $\gamma(\mathbf{q}_1, \dots, \mathbf{q}_{n_{node}})$ is invariant under the proper orthogonal group, then Cauchy's representation theorem (Truesdell & Noll [25, Sect. 11.] or Antman [1, Chapter 8]) implies that $\gamma(\mathbf{q})$ depends only on the set of quadratic invariants $\mathbb{I}(\mathbf{q}) = \mathbb{S}(\mathbf{q}) \cup \mathbb{T}(\mathbf{q})$, where

$$\begin{aligned}\mathbb{S}(\mathbf{q}) &= \{\mathbf{q}_A \cdot \mathbf{q}_B, 1 \leq A \leq B \leq n_{nodes}\} \\ \mathbb{T}(\mathbf{q}) &= \{\det([\mathbf{q}_A, \mathbf{q}_B]), 1 \leq A < B \leq n_{nodes}\}\end{aligned}\quad (57)$$

We first deal with the discrete strain energy function. Thereafter, we focus on the constraint functions emanating from the mortar contact formulation.

3.4 Treatment of the discrete strain energy function

Applying numerical integration to the evaluation of the discrete strain energy function (7) yields

$$V^{int}(\mathbf{q}) = \sum_{m=1}^{n_{gp}} \widetilde{W}(\boldsymbol{\pi}^{(m)}(\mathbf{q})) w^{(m)} \quad (58)$$

with

$$\boldsymbol{\pi}^{(m)}(\mathbf{q}) = \begin{bmatrix} C_{11}^{(m)}(\mathbf{q}) \\ C_{22}^{(m)}(\mathbf{q}) \\ C_{12}^{(m)}(\mathbf{q}) \end{bmatrix} \quad (59)$$

and the components of the discrete deformation tensor (5)

$$C_{ij}^{(m)}(\mathbf{q}) = \sum_{A,B=1}^{n_{node}} \mathbf{q}_A \cdot \mathbf{q}_B (\mathbf{e}_i \cdot \nabla N_A(\mathbf{X}^{(m)})) (\mathbf{e}_j \cdot \nabla N_B(\mathbf{X}^{(m)})) \quad (60)$$

In this connection, index m refers to specific quadrature points ($m \in \{1, \dots, n_{gp}\}$) with associated coordinates $\mathbf{X}^{(m)}$ and 'weights' $w^{(m)}$. It is obvious from (60), that the components of the discrete deformation tensor depend only on $\mathbb{S}(\mathbf{q})$ and thus qualify as invariants. With regard to (55), the discrete gradient of $V^{int}(\mathbf{q})$ can now be written as

$$\bar{\nabla}_q V^{int}(\mathbf{q}_n, \mathbf{q}_{n+1}) = \sum_{m=1}^{n_{gp}} D\boldsymbol{\pi}^{(m)}(\mathbf{q}_{n+\frac{1}{2}})^T \bar{\bar{\nabla}} \widetilde{W}(\boldsymbol{\pi}^{(m)}(\mathbf{q}_n), \boldsymbol{\pi}^{(m)}(\mathbf{q}_{n+1})) w^{(m)} \quad (61)$$

It is worth noting that $\bar{\bar{\nabla}} \widetilde{W}$ can be linked to the algorithmic constitutive relation proposed by Simo & Gonzalez [22, Section 4], see also Gonzalez [11].

4 Mortar method

In contrast to the collocation-type formulation of the contact constraints in the NTS approach, the mortar concept relies on the weak enforcement of the contact constraints. With regard to the semi-discrete formulation dealt with in Section 2.2, the discrete constraint functions $\Phi(\mathbf{q})$ corresponding to the mortar approach result from

$$\boldsymbol{\lambda} \cdot \Phi(\mathbf{q}) = \int_{\gamma_c} (\lambda \boldsymbol{\nu})^h \cdot (\mathbf{x}^{(1)h} - \mathbf{x}^{(2)h}) \, d\gamma \quad (62)$$

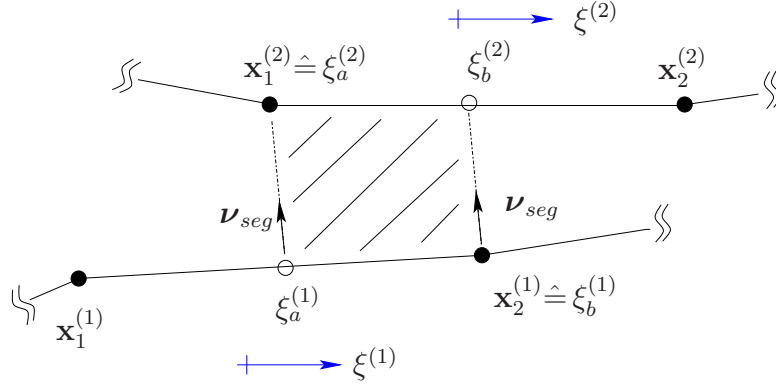


Figure 3: Representative mortar segment

To perform the integration along the contact curve γ_c , the notion of a contact segment can be employed. Originally, contact segments have been introduced by Simo et al. [24] to take into account the kinematics of the contact between two discretized bodies. Similar segmentation procedures have been devised by Papadopoulos & Taylor [19], McDevitt & Laursen [18] and Yang et al. [28].

In the following we consider a representative mortar segment depicted in Fig. 3. The relevant nodal position vectors lying on the boundaries of the two opposing elements may be collected in the vector

$$\mathbf{q}_{seg} = (\mathbf{x}_1^{(1)}, \mathbf{x}_2^{(1)}, \mathbf{x}_1^{(2)}, \mathbf{x}_2^{(2)}) \in \mathbb{R}^8 \quad (63)$$

To each mortar segment there correspond four coordinates $\xi_a^{(1)}$, $\xi_b^{(1)}$, $\xi_a^{(2)}$ and $\xi_b^{(2)}$, where $\xi^{(1)}$ and $\xi^{(2)}$ are local coordinates belonging to the opposing elements. For each segment a linear mapping $[-1, 1] \ni \eta \rightarrow \xi^{(\alpha)}$ of the form

$$\xi^{(\alpha)} = \frac{1}{2}(1 - \eta)\xi_a^{(\alpha)} + \frac{1}{2}(1 + \eta)\xi_b^{(\alpha)} \quad (64)$$

is introduced. This mapping can be used to parametrize the space finite element approximations of the Lagrange multipliers $(\lambda \boldsymbol{\nu})^h(\eta) = \lambda^h(\eta) \boldsymbol{\nu}_{seg}$, which characterize the normal contact forces. In this connection, $\boldsymbol{\nu}_{seg}$ is the unit outward normal to the segment which, in the present case, is constant. Specifically,

$$\lambda^h(\eta) = \sum_A N_A(\xi^{(1)}(\eta)) \lambda_A \quad (65)$$

The shape functions $N_A(\xi^{(1)})$ are inherited from the associated space finite element discretization. Similarly, the boundaries of the two opposing elements is given by

$$\begin{aligned} \mathbf{x}^{(1)h}(\eta) &= \sum_B N_B(\xi^{(1)}(\eta)) \mathbf{x}_B^{(1)} \\ \mathbf{x}^{(2)h}(\eta) &= \sum_C N_C(\xi^{(2)}(\eta)) \mathbf{x}_C^{(2)} \end{aligned} \quad (66)$$

Substituting from (65) and (66) into (62) yields the discrete constraint functions pertaining to the mortar contact formulation:

$$\Phi_A(\mathbf{q}) = \bigcup_{seg} \Phi_A^{seg}(\mathbf{q}_{seg}) \quad (67)$$

with the segment contributions

$$\Phi_A^{seq}(\mathbf{q}_{seg}) = \boldsymbol{\nu}_{seg} \cdot \left\{ \sum_B n_{AB}^{seq,(1)} \mathbf{x}_B^{(1)} - \sum_C n_{AC}^{seq,(2)} \mathbf{x}_C^{(2)} \right\} \quad (68)$$

and associated mortar integrals

$$\begin{aligned} n_{AB}^{seq,(1)} &= \int_{\gamma_c^{seg}} N_A^{(1)}(\xi^{(1)}(\eta)) N_B^{(1)}(\xi^{(1)}(\eta)) d\gamma \\ n_{AC}^{seq,(2)} &= \int_{\gamma_c^{seg}} N_A^{(1)}(\xi^{(1)}(\eta)) N_C^{(2)}(\xi^{(2)}(\eta)) d\gamma \end{aligned} \quad (69)$$

4.1 Mortar constraints in terms of invariants

We next aim at the parametrization of the mortar constraint functions (67) in terms of appropriate invariants. To this end it suffices to consider the segment contributions (68). Accordingly, we seek for reparametrizations of the form

$$\Phi_A^{seq}(\mathbf{q}_{seg}) = \tilde{\Phi}_A^{seq}(\boldsymbol{\pi}(\mathbf{q}_{seg})) \quad (70)$$

We illustrate our approach by considering the representative mortar segment depicted in Fig. 3. Accordingly, $A, B, C \in \{1, 2\}$ and the shape functions in (65), (66) and (69) are given by

$$\begin{aligned} N_1^{(\alpha)}(\xi^{(\alpha)}) &= \frac{1}{2}(1 - \xi^{(\alpha)}) \\ N_2^{(\alpha)}(\xi^{(\alpha)}) &= \frac{1}{2}(1 + \xi^{(\alpha)}) \end{aligned} \quad (71)$$

for $\alpha = 1, 2$. As indicated in Fig. 3, the filled circles correspond to nodal points, whereas the hollow circles are associated with orthogonal projections. Accordingly,

$$\begin{aligned} \xi_a^{(1)} &= \frac{2(\mathbf{x}_2^{(1)} - \mathbf{x}_1^{(1)}) \cdot (\mathbf{x}_1^{(2)} - \mathbf{x}_1^{(1)})}{\|\mathbf{x}_2^{(1)} - \mathbf{x}_1^{(1)}\|^2} - 1 & \xi_b^{(1)} &= 1 \\ \xi_b^{(2)} &= \frac{(2\mathbf{x}_2^{(1)} - \mathbf{x}_1^{(2)} - \mathbf{x}_2^{(2)}) \cdot (\mathbf{x}_2^{(1)} - \mathbf{x}_1^{(1)})}{(\mathbf{x}_2^{(2)} - \mathbf{x}_1^{(2)}) \cdot (\mathbf{x}_2^{(1)} - \mathbf{x}_1^{(1)})} & \xi_a^{(2)} &= -1 \end{aligned} \quad (72)$$

Upon introduction of the three quadratic invariants

$$\begin{aligned} \pi_1(\mathbf{q}_{seg}) &= (\mathbf{x}_2^{(1)} - \mathbf{x}_1^{(1)}) \cdot (\mathbf{x}_2^{(1)} - \mathbf{x}_1^{(1)}) \\ \pi_2(\mathbf{q}_{seg}) &= (\mathbf{x}_2^{(1)} - \mathbf{x}_1^{(1)}) \cdot (\mathbf{x}_1^{(2)} - \mathbf{x}_1^{(1)}) \\ \pi_3(\mathbf{q}_{seg}) &= (\mathbf{x}_2^{(1)} - \mathbf{x}_1^{(1)}) \cdot (\mathbf{x}_2^{(2)} - \mathbf{x}_1^{(1)}) \end{aligned} \quad (73)$$

the quantities in (72) may be recast in the form

$$\begin{aligned} \tilde{\xi}_a^{(1)} &= \frac{2\pi_2}{\pi_1} - 1 & \tilde{\xi}_b^{(1)} &= 1 \\ \tilde{\xi}_b^{(2)} &= \frac{\pi_1}{2\pi_1 - \pi_3 - \pi_2} & \tilde{\xi}_a^{(2)} &= -1 \end{aligned} \quad (74)$$

Accordingly, (64) can be alternatively written as

$$\tilde{\xi}^{(\alpha)} = \frac{1}{2}(1 - \eta)\tilde{\xi}_a^{(\alpha)} + \frac{1}{2}(1 + \eta)\tilde{\xi}_b^{(\alpha)} \quad (75)$$

Now, for $A = 1$, the segment contribution (68) is given by

$$\Phi_1^{seg} = \boldsymbol{\nu}_{seg} \cdot \left\{ n_{11}^{seg,(1)} \mathbf{x}_1^{(1)} + n_{12}^{seg,(1)} \mathbf{x}_2^{(1)} - (n_{11}^{seg,(2)} \mathbf{x}_1^{(2)} + n_{12}^{seg,(2)} \mathbf{x}_2^{(2)}) \right\} \quad (76)$$

Making use of (69) together with (71) and (75), the last equation yields

$$\begin{aligned} \Phi_1^{seg}(\mathbf{q}_{seg}) &= \frac{1}{4} \boldsymbol{\nu}_{seg} \cdot \left\{ (\mathbf{x}_1^{(1)} + \mathbf{x}_2^{(1)} - \mathbf{x}_1^{(2)} - \mathbf{x}_2^{(2)}) \int_{\gamma_c^{seg}} d\gamma \right. \\ &\quad + (-2\mathbf{x}_1^{(1)} + \mathbf{x}_1^{(2)} + \mathbf{x}_2^{(2)}) \int_{\gamma_c^{seg}} \tilde{\xi}^{(1)} d\gamma \\ &\quad + (\mathbf{x}_1^{(2)} - \mathbf{x}_2^{(2)}) \int_{\gamma_c^{seg}} \tilde{\xi}^{(2)} d\gamma \\ &\quad - (\mathbf{x}_1^{(2)} - \mathbf{x}_2^{(2)}) \int_{\gamma_c^{seg}} \tilde{\xi}^{(1)} \tilde{\xi}^{(2)} d\gamma \\ &\quad \left. - (\mathbf{x}_2^{(1)} - \mathbf{x}_1^{(1)}) \int_{\gamma_c^{seg}} (\tilde{\xi}^{(1)})^2 d\gamma \right\} \quad (77) \end{aligned}$$

Since, in the present case, the tangent vector

$$\frac{d\mathbf{x}^{(1)h}}{d\eta} = \frac{1}{4} (\mathbf{x}_2^{(1)} - \mathbf{x}_1^{(1)}) (\tilde{\xi}_b^{(1)} - \tilde{\xi}_a^{(1)}) \quad (78)$$

does not depend on η , the unit normal vector $\boldsymbol{\nu}_{seg}$ can be written as

$$\boldsymbol{\nu}_{seg} = -\mathbf{\Lambda} (\mathbf{x}_2^{(1)} - \mathbf{x}_1^{(1)}) / \|\mathbf{x}_2^{(1)} - \mathbf{x}_1^{(1)}\| \quad (79)$$

with the constant matrix

$$\mathbf{\Lambda} = \begin{bmatrix} 0 & 1 \\ -1 & 0 \end{bmatrix} \quad (80)$$

Note that $\mathbf{\Lambda}^T = \mathbf{\Lambda}^{-1} = -\mathbf{\Lambda}$ and $\mathbf{\Lambda}^2 = -\mathbf{I}_2$. Let two additional quadratic invariants be defined by

$$\begin{aligned} \pi_4(\mathbf{q}_{seg}) &= (\mathbf{x}_2^{(1)} - \mathbf{x}_1^{(1)}) \cdot \mathbf{\Lambda} (-2\mathbf{x}_1^{(1)} + \mathbf{x}_1^{(2)} + \mathbf{x}_2^{(2)}) \\ \pi_5(\mathbf{q}_{seg}) &= (\mathbf{x}_2^{(1)} - \mathbf{x}_1^{(1)}) \cdot \mathbf{\Lambda} (\mathbf{x}_1^{(2)} - \mathbf{x}_2^{(2)}) \end{aligned} \quad (81)$$

Employing the invariants (73) and (81), and taking into account the skew-symmetry of $\mathbf{\Lambda}$ as well as the relationship

$$d\gamma = \frac{1}{4} \|\mathbf{x}_2^{(1)} - \mathbf{x}_1^{(1)}\| (\tilde{\xi}_b^{(1)} - \tilde{\xi}_a^{(1)}) \quad (82)$$

which is consistent with (78), a straightforward calculation shows that constraint function (77) can be recast as

$$\tilde{\Phi}_1^{seg}(\boldsymbol{\pi}(\mathbf{q}_{seg})) = \frac{1}{16} (\tilde{\xi}_b^{(1)} - \tilde{\xi}_a^{(1)}) \left\{ \pi_4 \int_{-1}^1 (\tilde{\xi}^{(1)} - 1) d\eta + \pi_5 \int_{-1}^1 (\tilde{\xi}^{(2)} - \tilde{\xi}^{(1)} \tilde{\xi}^{(2)}) d\eta \right\} \quad (83)$$

Note that, with regard to (75) and (74), the evaluation of the integrals in (83) can be easily accomplished.

For $A = 2$, the segment contribution (68) can be calculated along the same lines as before for $A = 1$ and yields

$$\tilde{\Phi}_2^{seq}(\boldsymbol{\pi}(\mathbf{q}_{seg})) = \frac{1}{16}(\tilde{\xi}_b^{(1)} - \tilde{\xi}_a^{(1)}) \left\{ \pi_5 \int_{-1}^1 (\tilde{\xi}^{(2)} + \tilde{\xi}^{(1)}\tilde{\xi}^{(2)}) d\eta - \pi_4 \int_{-1}^1 (\tilde{\xi}^{(1)} + 1) d\eta \right\} \quad (84)$$

It is easy to see that the invariants in (73) depend on \mathbb{S} . Moreover, since $\mathbf{a} \cdot \boldsymbol{\Lambda} \mathbf{b} = \det([\mathbf{a}, \mathbf{b}])$ for any $\mathbf{a}, \mathbf{b} \in \mathbb{R}^2$, the invariants in (81) depend on \mathbb{T} .

It is important to realize that in addition to being rotationally invariant, the quadratic invariants in (73) and (81) are as well invariant under translations. It can be easily verified that

$$\pi_i(\mathbf{x}_1^{(1)} + \mathbf{c}, \mathbf{x}_2^{(1)} + \mathbf{c}, \mathbf{x}_1^{(2)} + \mathbf{c}, \mathbf{x}_2^{(2)} + \mathbf{c}) = \pi_i(\mathbf{x}_1^{(1)}, \mathbf{x}_2^{(1)}, \mathbf{x}_1^{(2)}, \mathbf{x}_2^{(2)}) \quad (85)$$

for $i = 1, \dots, 5$ and any $\mathbf{c} \in \mathbb{R}^2$. Translational invariance of the augmented Hamiltonian is associated with conservation of the total linear momentum.

We finally remark that the above reparametrization of the contact constraints in conjunction with the (discrete) gradient also turned out to be beneficial to the computer implementation. Similar observations have been made in the framework of the NTS method, see Betsch & Hesch [5].

5 Numerical example

The numerical example consists of the planar model of a bearing depicted in Fig. 4. The bearing consists of two rings (Young's modulus $E = 10^5$, Poisson's ratio $\nu = 0.1$ and mass density $\varrho_R = 0.001$), which are discretized by 4-node isoparametric displacement-based plain strain elements. The discretization of the outer ring relies on 10x48 elements, for the inner ring 10x40 have been used.

The motion of the inner ring is restricted by the condition of persistent contact with the outer ring. Pure Dirichlet-type conditions are applied to fix the outer boundary of the outer ring. To get a pre-stressed initial configuration of the whole bearing, a static equilibrium problem is solved first. To this end the initial outer diameter of the inner ring¹ ($d_i = 80.1$) exceeds the initial inner diameter of the outer ring² $d_o = 80.0$. Accordingly, the static equilibrium problem consists of enforcing (frictionless) contact between inner and outer ring. The static equilibrium problem is solved in one load increment.

After the solution of the equilibrium problem the transient calculation proceeds with $\Delta t = 0.01$. For $t \in [0, 0.5]$, a torque acts on the inner ring in form of a hat function over time. Then, for $t \in (0.5, 2]$, no external loads are acting on the bearing anymore. Fig. 5 shows that for $t \geq 0.5$ the present scheme does indeed conserve the total energy for the frictionless contact problem under consideration. In addition to that, Fig. 6 corroborates algorithmic conservation of angular momentum.

¹the inner diameter is 50

²the outer diameter is 100

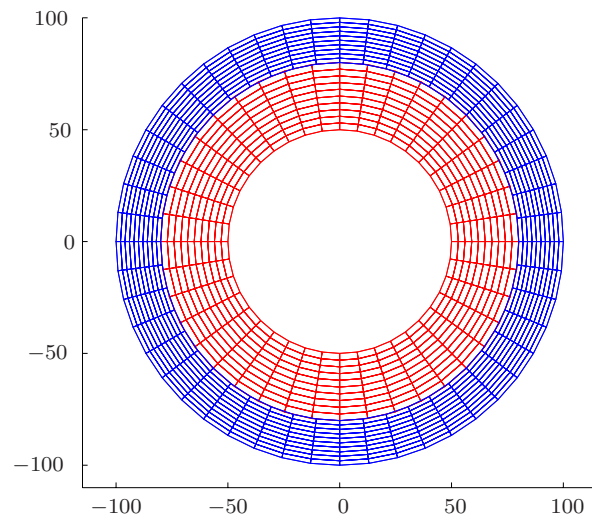


Figure 4: Discretized bearing

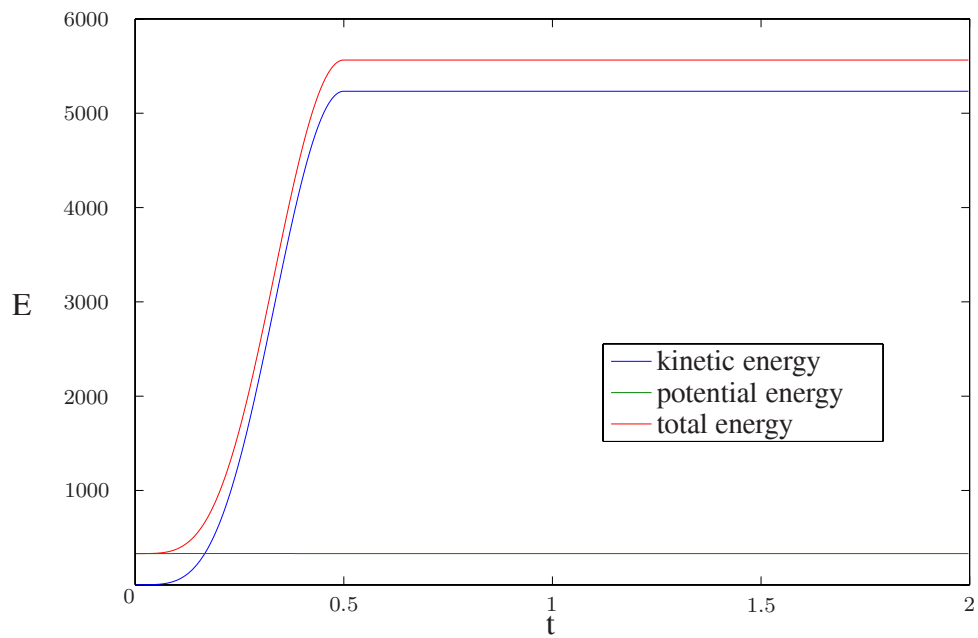


Figure 5: Energy versus time

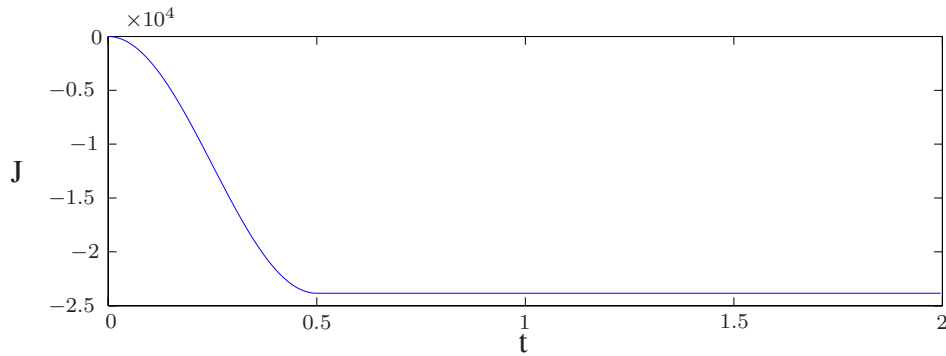


Figure 6: Total angular momentum versus time

6 Conclusions

The main new contribution of the present work lies in the design of the algorithmic contact forces within the framework of the mortar formulation. In particular, the newly-proposed parametrization of the mortar contact constraints in terms of appropriate invariants along with the use of the notion of a discrete gradient are the main features which facilitate the design of an energy-momentum scheme. Interestingly, the reparametrization of the contact constraints also greatly simplifies the computer implementation of the mortar formulation.

REFERENCES

- [1] S.S. Antman. *Nonlinear Problems of Elasticity*. Springer-Verlag, 2nd edition, 2005.
- [2] F. Armero and E. Petöcz. Formulation and analysis of conserving algorithms for frictionless dynamic contact/impact problems. *Comput. Methods Appl. Mech. Engrg.*, 158:269–300, 1998.
- [3] O.A. Bauchau and C.L. Bottasso. On the design of energy preserving and decaying schemes for flexible, nonlinear multi-body systems. *Comput. Methods Appl. Mech. Engrg.*, 169:61–79, 1999.
- [4] P. Betsch. The discrete null space method for the energy consistent integration of constrained mechanical systems. Part I: Holonomic constraints. *Comput. Methods Appl. Mech. Engrg.*, 194(50-52):5159–5190, 2005.
- [5] P. Betsch and C. Hesch. Energy-momentum conserving schemes for frictionless dynamic contact problems. Part I: NTS method. IUTAM Bookseries, Springer-Verlag, in print.
- [6] P. Betsch and P. Steinmann. Conservation properties of a time FE method. Part II: Time-stepping schemes for nonlinear elastodynamics. *Int. J. Numer. Methods Eng.*, 50:1931–1955, 2001.
- [7] P. Betsch and P. Steinmann. Conservation properties of a time FE method. Part III: Mechanical systems with holonomic constraints. *Int. J. Numer. Methods Eng.*, 53:2271–2304, 2002.
- [8] C.W. Gear, G.K. Gupta, and B.J. Leimkuhler. Automatic integration of the Euler-Lagrange equations with constraints. *J. Comp. Appl. Math.*, 12:77–90, 1985.

- [9] O. Gonzalez. Time integration and discrete Hamiltonian systems. *J. Nonlinear Sci.*, 6:449–467, 1996.
- [10] O. Gonzalez. Mechanical systems subject to holonomic constraints: Differential-algebraic formulations and conservative integration. *Physica D*, 132:165–174, 1999.
- [11] O. Gonzalez. Exact energy and momentum conserving algorithms for general models in nonlinear elasticity. *Comput. Methods Appl. Mech. Engrg.*, 190:1763–1783, 2000.
- [12] O. Gonzalez and J.C. Simo. On the stability of symplectic and energy-momentum algorithms for non-linear Hamiltonian systems with symmetry. *Comput. Methods Appl. Mech. Engrg.*, 134:197–222, 1996.
- [13] S. Hübner and B.I. Wohlmuth. A primal-dual active set strategy for non-linear multibody contact problems. *Comput. Methods Appl. Mech. Engrg.*, 194:3147–3166, 2005.
- [14] T.A. Laursen. *Computational contact and impact mechanics*. Springer-Verlag, 2002.
- [15] T.A. Laursen and V. Chawla. Design of energy conserving algorithms for frictionless dynamic contact problems. *Int. J. Numer. Methods Eng.*, 40:863–886, 1997.
- [16] T.A. Laursen and G.R. Love. Improved implicit integrators for transient impact problems—geometric admissibility withing the conserving framework. *Int. J. Numer. Methods Eng.*, 53:245–274, 2002.
- [17] J.E. Marsden and T.S. Ratiu. *Introduction to Mechanics and Symmetry*. Springer-Verlag, 2nd edition, 1999.
- [18] T.W. McDevitt and T.A. Laursen. A mortar-finite element formulation for frictional contact problems. *Int. J. Numer. Methods Eng.*, 48:1525–1547, 2000.
- [19] P. Papadopoulos and R.L. Taylor. A mixed formulation for the finite element solution of contact problems. *Comput. Methods Appl. Mech. Engrg.*, 94:373–389, 1992.
- [20] M.A. Puso and T.A. Laursen. A mortar segment-to-segment contact method for large deformation solid mechanics. *Comput. Methods Appl. Mech. Engrg.*, 193:601–629, 2004.
- [21] J.C. Simo. Numerical analysis and simulation of plasticity. In P.G. Ciarlet and J.L. Lions, editors, *Handbook of Numerical Analysis*, volume VI, pages 183–499. Elsevier Science B.V., 1998.
- [22] J.C. Simo and O Gonzalez. Recent results on the numerical integration of infinite-dimensional Hamiltonian systems. In T.J.R. Hughes, E. Onate, and O.C. Zienkiewicz, editors, *Recent developments in finite element analysis*, pages 255–271. CIMNE, Barcelona, 1994.
- [23] J.C. Simo and N. Tarnow. The discrete energy-momentum method. Conserving algorithms for nonlinear elastodynamics. *Z. angew. Math. Phys. (ZAMP)*, 43:757–792, 1992.
- [24] J.C. Simo, P. Wriggers, and R.L. Taylor. A perturbed Lagrangian formulation for the finite element solution of contact problems. *Comput. Methods Appl. Mech. Engrg.*, 50:163–180, 1985.

- [25] C. Truesdell and W. Noll. *The Non-Linear Field Theories of Mechanics*. Springer-Verlag, 3rd edition, 2004.
- [26] B.I. Wohlmuth. *Discretization Methods and Iterative Solvers based on Domain Decomposition*. Springer Verlag, 2000.
- [27] P. Wriggers. *Computational contact mechanics*. John Wiley & Sons, 2002.
- [28] B. Yang, T.A. Laursen, and X.N. Meng. Two dimensional mortar contact methods for large deformation frictional sliding. *Int. J. Numer. Methods Eng.*, 62:1183–1225, 2005.